AIAA 80-0791R

Experimental and Theoretical Study of Nonlinear Flutter

Samuel C. McIntosh Jr.,* Robert E. Reed Jr.,† and William P. Rodden‡
Nielsen Engineering and Research, Inc., Mountain View, Calif.

A "typical-section" flutter model, incorporating linear and nonlinear spring restraints in torsion and plunge, has been designed, built, and tested in a wind tunnel. The principal goal of the experiments was to produce high-quality stability and response data, for a number of different types of nonlinearities, from a model whose properties are known very accurately. An additional goal was to develop and validate an accurate mathematical model of the system to aid in theoretical studies. Experiments were performed for both hardening and softening springs in plunge, and hardening springs in torsion. Both limit-cycle and divergent amplitude-sensitive instabilities were observed. The experimental results and some comparisons with theoretical nonlinear time-history calculations and linear stability analyses are described. Generally excellent agreement was obtained between linear experimental and theoretical results, and an amplitude-sensitive instability was predicted theoretically that agreed with experimental observations. Comments are also given concerning improvements to be made to the theoretical model and additional theoretical and experimental work to be done.

Introduction

IN the development of analytical techniques to treat aeroelastic problems, the assumption of linearity has understandably been dominant. However, there are many instances where nonlinearities can be important, and where an understanding of their effects is crucial to an efficient and safe design. Nonlinearities can be characterized as either distributed or concentrated,[1] according to their origin. Distributed nonlinearities arise from slippage in riveted joints or from buckling in a built-up structure, for example, whereas concentrated nonlinearities are associated with such localized phenomena as backlash, free play, or saturation in non-powered and powered controls. These latter nonlinearities are generally the most important. Missile control surfaces that are designed to be easily attached or removed, all-movable aircraft lifting surfaces such as horizontal tails, or rotatable pylons on variable-sweep aircraft all exhibit nonlinear behavior that can be potentially dangerous from an aeroelastic viewpoint. An excellent discussion of structural nonlinearities in aircraft is contained in Ref. 1, along with a summary of both experimental and theoretical techniques employed to evaluate their effects. The situation with regard to missiles is summarized in Ref. 2.

Aside from direct numerical simulation, the principal theoretical technique that has been applied is the well-known describing-function technique,[3] which is an adaptation of the method of harmonic balance to treat concentrated nonlinearities, such as nonlinear controls or root restraints. In this technique sinusoidal motion of the structure is assumed, and the load developed at the control or at the structural root restraint is expanded in a Fourier series. All harmonics but the fundamental are neglected, and the ratio of the fundamental harmonic of the load to the assumed displacement is used to define an "equivalent" linear spring. The "equivalent" linear system is then analyzed by conventional means. While this technique has been widely used, it does have certain limitations. Expressions for the equivalent linear property have to be derived for each type of nonlinearity, and the method becomes unwieldy when a number of nonlinearities have to be treated simultaneously, or when the nonlinearities involve a large number of degrees of freedom. Direct numerical simulation has also proved useful. However, it can be difficult to interpret a time history properly, or to obtain quantitative measures of the stability characteristics of the system. A recent theoretical study of the describing-function technique as applied to a missile control surface is described in Ref. 4.

Apparently, very little has been done to study nonlinear effects on flutter experimentally. Some recent European experiments on a wing with a nonlinear aileron restraint are discussed in Ref. 1. In the United States, experiments on a typical-section flutter model with pitch free play are described in Ref. 5. The experimental results were verified by numerical simulation on an analog computer, and other types of nonlinearities in pitch were also studied on the computer.

The purpose of the present work was to extend the types of nonlinearities treated experimentally and to develop an experimental model that was capable of producing high-quality nonlinear aeroelastic response and stability data. In addition, it was desired to produce a model that could be represented very accurately theoretically, so as to permit meaningful theoretical/experimental comparisons and to provide data for evaluating new theoretical techniques for treating nonlinear aeroelastic problems.

This paper deals principally with an experimental investigation. A two-dimensional typical-section flutter model, similar to a linear one tested at Stanford University,[6] was designed and tested in the Nielsen Engineering and Research, Inc. (NEAR) Water/Wind Tunnel. The model design and instrumentation are discussed briefly. Results from the nonlinear tests, which include both subcritical response and stability data, are described in detail. Theoretical time histories of nonlinear model response have been computed for comparison with the experimental data, and these are also described. References 7 and 8 contain a more detailed description of this work.

Description of Model and Tunnel

Model Design

A principal goal of the model design was to produce a linear system that could be easily modified to introduce specific nonlinear properties with minimal changes in the other parameters of the basic system. Under this concept, the properties of the basic linear system could be determined, and changes in the system characteristics for nonlinear con-

Presented as Paper 80-0791 at the AIAA/ASME/ASCE/AHS 21st Structures, Structural Dynamics and Materials Conference, Seattle, Wash., May 12-14, 1980; submitted June 12, 1980; revision received May 4, 1981.

*Project Manager, Structures. Associate Fellow AIAA.

†Research Engineer.

‡Consultant. Associate Fellow AIAA.

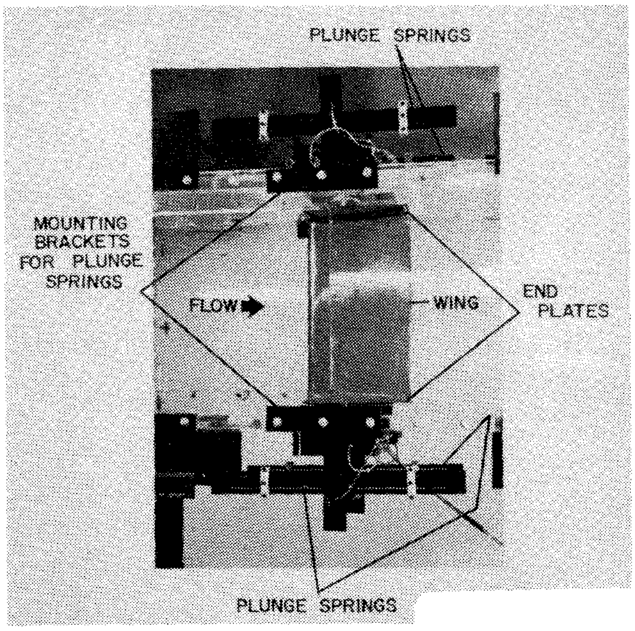

Fig. 1 Wing installed in tunnel.

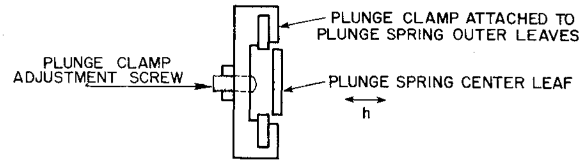

Fig. 2 Cross-section view of plunge spring illustrating operation of plunge clamp.

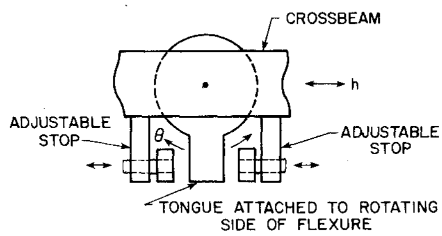

Fig. 3 Side view of model illustrating operation of pitch spring stops.

figurations could be attributed to the introduction of specific nonlinearities.

The basic linear system is a rectangular wing with an NACA 0012 airfoil. It has degrees of freedom in pitch and plunge. A picture of the model in the NEAR Water/Wind Tunnel is shown in Fig. 1. (Plunge clamps are installed on the plunge springs. These are discussed below.) Rectangular end plates on the wing are used to minimize tip effects. Separation at the juncture of the wing and the tip plates was reduced by forming the inboard portion of each tip plate to the wing profile.

The wing is composed of an aluminum spar (the pitch axis of rotation) with ribs imbedded in foam that was formed to the proper airfoil shape and covered with a layer of fiberglas. The spar protrudes through holes in the top and bottom tunnel walls and is attached to the pitch springs. These, in turn, are attached to crossbeams which are fixed to the middle leaves of the plunge springs. The outer leaves of the plunge springs are rigidly mounted to the tunnel walls at the centers of the springs.

The pitch springs are commercially available flexure pivots that allow ±7.5 deg of rotation through the elastic bending of thin rectangular flexures. The plunge springs have a flexural length of twice their apparent length (see Fig. 1) since the ends are free to deflect, thereby allowing the outer leaves to deflect. Because the free ends can move as the spring deflects, the spring retains its linear characteristics over large displacements. Also, there are no sliding surfaces at support points which would produce damping. The springs were designed to deflect elastically approximately 0.50 in. Reference 7 gives additional details concerning the spring design.

The linear system was modified by introducing nonlinearities into the spring rates. Three devices were used to produce the following nonlinearities: 1) plunge screws—nonlinear hardening plunge spring (curved force-displacement relation); 2) plunge clamps—either bilinear hardening or bilinear softening plunge springs; 3) pitch stops—bilinear hardening pitch spring.

The plunge clamps are attached to the outer leaves of the plunge springs (see Fig. 1). They produce either a hardening or softening nonlinearity depending on whether a gap or a preload is used. A gap or a preload is determined by the position of the adjustment screw in the center of the clamp relative to the center leaf of the plunge spring. The softening spring rate is produced by equally preloading each of the eight clamps. When the spring deflects a certain amount, one side (two springs) loses contact with the adjustment screws, and these spring rates return to their softer linear value. With the reverse deflection, the other side loses its preload. With a gap rather than a preload, the spring has the unmodified linear spring rate until the deflection exceeds the gap. The spring rate for displacements larger than the gap then includes the effect of the stop, which increases the stiffness of the spring. This is illustrated in Fig. 2. The plunge screws, which work similarly to the plunge clamps, are mounted in pairs to a rigid bar attached to the tunnel wall.

For the pitch hardening nonlinearity, a tongue was bolted to the rotating side of each flexure pivot, and movable stops were attached to the crossbeams. When the model pitched enough to force the tongue against one of the stops, the pitch

Table 1 Summary of properties of linear model

Total weight	11.93 lb
Total mass, M_T	0.03089 lb-s^2/in.
Mass of rotating components, M_θ	0.01522 lb-s^2/in.
Mass of rack assembly, M_r	3.883×10^{-4} lb-s^2/in.
Rack assembly c.g. offset, e	1.1 in.
Wing span, s	18 in.
Wing chord, $c = 2b$	9.90 in.
Wing area, $S = cs$	178.2 in.^{2}
Distance from wing leading edge to pitch axis	3.48 in.
Distance from pitch axis aft to c.g. of rotating components, X_θ	0.77 in.
Moment of inertia of rotating components about pitch axis, I_θ	0.0972 lb-in.-s^2
Plunge stiffness, K_h	125 lb/in.
Pitch stiffness, K_θ	776 in.-lb/rad
Plunge uncoupled natural frequency, f_h	10.1 Hz (calculated) 10.4 Hz (measured)
Pitch uncoupled natural frequency, f_θ	14.2 Hz (calculated) 14.0 Hz (measured)
Coupled natural frequencies, f_1 and f_2 (calculated)	9.90 Hz, 14.9 Hz
Damping coefficient in plunge and pitch, γ (measured)	0.009
Slope of lift curve, C_{ℓ_α} (measured)	6.76
Slope of moment curve, about pitch axis, C_{m_α} (measured)	0.783
Center of pressure location (in chords) aft of leading edge, ξ (measured)	0.236
Total mass, M_T, plunge clamp at location C[a]	0.03457 lb-s^2/in.
Total mass, M_T, plunge clamp at location D[a]	0.03393 lb-s^2/in.

[a] Mass of pitch stops and holders included.

spring rate was increased by an amount governed by the bending stiffness of the stop. The tongue and stops were installed on both ends of the model so as to minimize the excitation of differential pitch motions. This is illustrated in Fig. 3.

A summary of the properties of the basic linear model is given in Table 1.

Tunnel

The basic test section of the NEAR Water/Wind Tunnel is all plexiglas for complete visibility. It is $14 \times 20 \times 72$ in. long. The nozzle, test section, and diffuser can be rotated as a unit, making the test section either 14 or 20 in. high. Flow speed ranges are 0-20 ft/s in water and 0-200 ft/s in air. Flow angle deviation in the test section is ± 0.2 deg, and the velocity deviation is $\pm 0.2\%$ maximum. There are four turbulence-damping screens in the settling chamber.

Measurement and Calculation of System Properties

In the determination of inertia properties, care was taken to incorporate properly the contributions of all model components. This included computing the effective mass of the plunge springs and accounting for the inertia of the plunge clamps, which depended on where they were installed.

The plunge clamps and pitch stops produced bilinear spring characteristics. The measured low- and high-amplitude spring constants are given in Table 2 for the configurations tested. The actual amplitude at which the spring rate transitions from one value to the other is governed by the gap or preload set with the pitch stops.

The damping in the system was estimated by computing logarithmic decrements from single-degree-of-freedom free decay records in pitch and plunge. One source of damping not accounted for is the rack and pinion used to convert pitch angular rotation for measurement. The damping from this source is believed to be negligible.

Aerodynamic Properties

The static lift and moment characteristics were measured from model static response as a function of tunnel speed, with an initial pitch angle introduced. During these tests, a linear plunge-displacement variation with dynamic pressure at zero pitch angle was observed. The origin of this phenomenon is at present unknown; it may be the result of some combination of model misalignment or asymmetry. Fortunately, this bias remained quite repeatable throughout the tests, so it was possible to remove it from the experimental data. The theoretical wall correction[6] for the linear two-dimensional lift-curve slope gives a value of 7.57. The lower value measured (6.76; see Table 1) is in all likelihood the result of the lack of true two-dimensional flow over the total span of the model. (Note that there is a gap between the end plates and the walls; see Fig. 1.)

In addition to the static aerodynamic parameters, there are dynamic parameters that are also affected by the tunnel walls and spanwise induction. The theoretical model for this system (see Refs. 7 and 8) incorporates a two-term exponential approximation to the Wagner indicial function in the unsteady aerodynamic terms. With this approximation, the Duhamel integrals expressing aerodynamic loads for arbitrary motion can be replaced by differential equations, in an approach similar to that of Rodden and Stahl[9] for a single strip. The parameters in the approximation to the Wagner function should be different from their theoretical free-air values in order to reflect the experimental conditions. There are some apparent-mass aerodynamic terms that are also affected. In the calculations discussed here, free-air values for these parameters were used. Future work will involve estimating these parameters from experimental data.

Table 2 Summary of bilinear spring rates. Stiffnesses in lb/in. for plunge, in.-lb/rad for pitch

Configuration	Stiffness Low amplitude	Stiffness High amplitude
Plunge clamps, location C,[a] hardening	125	194
Plunge clamps, location C, softening	288	194
Plunge clamps, location D,[b] hardening	125	256
Plunge clamps, location D, softening	417	256
Pitch stiffening spring	776	1294

[a] 2.75 in. from end of plunge spring. [b] 3.75 in. from end of plunge spring.

Instrumentation

In order to avoid difficulties with integrating or differentiating experimental data, it was decided to measure independently displacement and velocity in each degree of freedom. To eliminate effects caused by differential plunge and pitch between the ends of the model, two transducers for each variable were used, one at each end, and their outputs were averaged electronically. Difference signals could also be obtained to measure model differential motion. The final output therefore consisted of four channels of data—plunge (h), plunge velocity ($\dot{h}$), pitch (θ), and pitch velocity ($\dot{\theta}$)—from eight transducers. Linear displacement and velocity transducers were used; pitch rotation was converted to linear motion with a rack and pinion gear at each end of the model.

The four channels of model data, plus tunnel dynamic pressure, were recorded in analog form on tape. The model data were also passed to a strip-chart recorder for real-time viewing during the tests.

Dynamic Tests

Data Records

Time histories of displacement and velocity for both pitch and plunge were recorded in both linear and nonlinear tests. All of the data records taken are being preserved and will be available for further analysis. Additional details concerning these data may be obtained from the authors. All test conditions and model configurations for which data are available are summarized in Ref. 7; representative tests are discussed here.

Linear Tests

Subcritical response data were also taken in addition to determining the flutter speed. Since the turbulence level in the tunnel was relatively low, it was often necessary to pluck the model gently in plunge by pushing on the plunge springs in order to excite flutter. As is usual in tests of this nature, precise determination of the flutter speed was difficult. Generally, the flutter speed was taken to be the lowest speed that resulted in clearly divergent motion. As soon as divergent motion was established, the model was stabilized by restraining the plunge motion by hand. The primary concern here was to prevent the pitch amplitude from exceeding the

Table 3 Measured linear flutter characteristics

Test	Configuration	Speed, ft/s	Frequency, Hz	Comments
4	Linear model	133	11.7	Basic linear model
11	Plunge clamps, location C, "infinite" gap	138	11.3	Linear model with added mass
17	Plunge clamps, location D, "infinite" gap	136	11.4	Linear model with added mass

Table 4 Measured nonlinear flutter characteristics. Limit and initial amplitudes given as equivalent displacement at gap locations

Test	Configuration	Gap, in.	Speed, ft/s	Frequency, Hz	Limit amplitude, in.[a]	Comments
						Clamps at location C
12	Plunge clamps	0.002	111	12.7	0.002	Hardening spring
			118	12.4	∞	
						Plucked to start:
13		0.010	116	12.0	∞	0.046 in.
			125	12.1	∞	0.034 in.
			128	12.1	∞	0.030 in.
			132	11.8	∞	0.024 in.
14		−0.006	108	13.9	0.007	Softening spring
		(preload)	111	13.9	0.009	
			113	13.8	0.011	
			119	13.8	0.013	
15		−0.014	117	14.3	0.0011	Softening spring
		(preload)	124	14.3	0.0075	
			128	14.3	0.010	
			131	14.3	0.012	
			135	14.3	0.013	
						Clamps at location D
18		0.002	105	13.8	0.003	Hardening spring
			108	13.7	0.012	
			111	13.8	0.015	
						Plucked to start:
20		0.010	117	13.0	0.033	0.046 in. stable; 0.066 in. unstable
			122	13.6	0.050	0.036 in. stable; 0.046 in. unstable
19		−0.002	117	14.5	0.002	No pluck
		(preload)	119	14.5	0.016	Pluck 0.056 in.
			122	14.3	0.019	Pluck 0.036 in.
			127	14.3	0.020	No pluck
22	Pitch stiffener	0.010	136	11.8	0.012	Pitch limit amplitude
			141	11.9	0.016	
23		0.020	135	11.7	0.024	Pitch limit amplitude
			140	12.1	0.028	

[a] ∞ means model diverged until it had to be restrained to avoid damage.

elastic limit of the torsion springs ($\approx$7.5 deg). The measured linear flutter characteristics are summarized in Table 3. Note that linear flutter speeds were also determined for the plunge clamps in locations C and D by setting very large gaps between the adjustable screws and the center leaves of the plunge springs.

Nonlinear Tests

For the nonlinear configurations, different types of instabilities can occur. For example, there can be a stable limit cycle, where the model oscillates at a constant amplitude and frequency. Or, there can be a divergent amplitude-sensitive instability, where the model is stable for initial amplitudes below a given value but is divergent if the initial amplitude exceeds that value. In addition to obtaining subcritical response data and critical airspeeds, it was therefore also necessary to determine the type of instability that occurred. Additional measurements for these instabilities were then the initial plunge amplitude necessary to excite flutter, or the flutter limit-cycle amplitude, or both. These measurements are included in the summary of nonlinear flutter characteristics in Table 4. The limit amplitudes shown have been converted from the physical values measured to the equivalent displacements at the gap location, in order to permit direct comparison of these amplitudes with the gap setting. An infinite limit amplitude means that the motion was divergent, at least to the point where the model had to be restrained to avoid damage.

Discussion of Results

For the nonlinear configurations involving bilinear spring rates, much information can be obtained from determining the linear stability characteristics at both spring rates. These linear characteristics will be representative of the nonlinear behavior at the limits of small and large amplitudes. Linear flutter analyses were performed for all possible combinations of bilinear spring rates and values of total mass M_T that could result from the nonlinear configurations tested. The results of these calculations are given in Table 5.

Cases 1A-1C represent the basic linear system and the system with infinite-gap plunge clamps at locations D and C, respectively. The remaining cases represent the various combinations of spring rates obtainable at either large or small amplitudes with the bilinear springs. As an example of what can be inferred from these results, consider cases 2 and 4 for a softening plunge spring, with the plunge clamp at location C. For small plunge amplitudes, the plunge stiffness is 288 lb/in., and the predicted flutter speed is 122 ft/s. At very large plunge amplitudes, where the displacement at the plunge-clamp locations is much greater than that needed to overcome the preload, linear behavior is also approached, with the lower plunge stiffness of 194 lb/in. and a predicted flutter speed of 117 ft/s. These figures suggest that at speeds above 117 ft/s, an amplitude-dependent instability could exist. Whether this instability is a stable or unstable limit cycle cannot necessarily be inferred, however, although it is tempting to come to the conclusion that the limit cycle should be unstable, since increased amplitudes produce "equivalent" linear stiffness values with presumably lower and lower flutter speeds. The same hypothesis can be made for the softening spring at location D, except that the predicted flutter speeds for the two limiting cases differ much more—from 200 to 116 ft/s. Similar arguments can be made for the hardening plunge-spring cases, where the large-amplitude flutter speeds are much lower than the small-amplitude speeds. (For the hardening springs, the low-amplitude configurations are the linear system with the nominal spring rates and the increased

Table 5 Calculated linear flutter characteristics

Case	K_h, lb/in.	K_θ, in.-lb/rad	Mass, lb-s^2/in.	Flutter speed, ft/s	Flutter frequency, Hz	Description of configuration
1A	125	776	0.0309	131	11.1	Linear system
1B	125	776	0.0339	137	10.8	Linear system, plunge clamp at location D
1C	125	776	0.0346	139	10.7	Linear system, plunge clamp at location C
2	288	776	0.0346	122	14.7	Small amplitude of plunge softening spring; clamp at location C
3	417	776	0.0339	200	17.2	Small amplitude of plunge softening spring; clamp at location D
4	194	776	0.0346	117	12.5	Large amplitude of plunge softening and hardening springs; clamp at location C
5	256	776	0.0339	116	14.2	Large amplitude of plunge softening and hardening springs; clamp at location D
6	125	1294	0.0331	211	11.5	Large amplitude of pitch hardening spring; plunge clamps removed

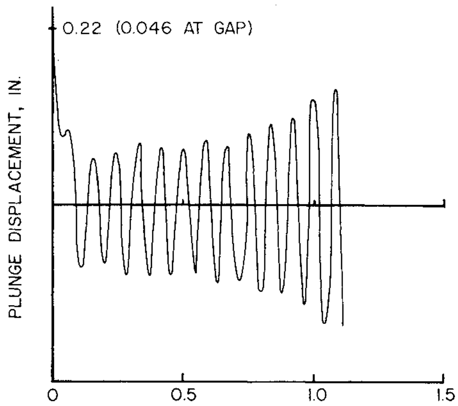

Fig. 4 Chart recording of divergent nonlinear flutter, $V = 116$ ft/s, test 13 (see Table 4).

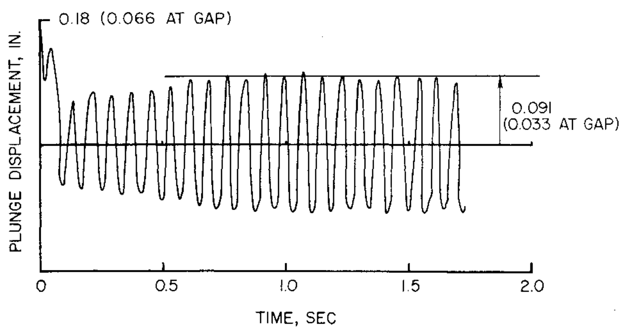

Fig. 5 Chart recording of nonlinear limit-cycle flutter, $V = 117$ ft/s, test 20 (see Table 4).

total mass—cases 1B and 1C.) In contrast to the plunge-spring nonlinearities, the large-amplitude linear analysis for the pitch hardening spring shows a much higher flutter speed than that for small amplitudes – 211 ft/s. This suggests that at speeds above 137 ft/s, a stable limit cycle should be observed.

In light of the above observations, it is interesting now to examine the experimental results, as summarized in Tables 3 and 4. First, let us consider the linear systems. For the nominal linear system, the theoretical values (case 1A in Table 5) are 131 ft/s for the flutter speed and 11.1 Hz for the flutter frequency. The corresponding experimental values are 133 ft/s and 11.7 Hz (test 4, Table 3). For the plunge clamps at locations C and D, the experimental values (tests 11 and 17, respectively) agree equally well with the theoretical values (cases 1C and 1B, respectively). For all of these configurations, the disagreement in flutter frequency is larger than that for the flutter speed. However, the same trends are observed in both cases—increasing flutter speeds and lower flutter frequencies with increasing total mass.

For the hardening plunge spring with the clamp at location C, the experimental results are summarized by the data for tests 12 and 13. In test 12, with a very small gap, incipient flutter was observed at 111 ft/s, and divergent flutter at 118 ft/s with a frequency of 12.4 Hz. With a gap of only 0.002 in., this system could be expected to exhibit behavior similar to that of a linear system with the large-amplitude stiffness value, as soon as its motion produces amplitudes at the gap location that exceed significantly 0.002 in. This is case 4 in Table 5, and both the flutter speed and frequency agree very well with the experimental values. With a larger gap (test 13), a divergent amplitude-sensitive instability was observed. At an airspeed of 116 ft/s, which is near the theoretical linear large-amplitude flutter speed, a relatively large initial amplitude is required to cause the instability, and the frequency is near the calculated linear-system frequency. As the airspeed is increased toward the theoretical linear small-amplitude flutter speed, the initial amplitude required to induce flutter is decreased, and the frequency exhibits a tendency to decrease toward the calculated frequency, at least up to the highest airspeed tested of 132 ft/s.

With the clamp at location D, the linear large-amplitude flutter speed is virtually identical to that for the clamp at location C (cases 4 and 5 in Table 5), even though the stiffness for the former is considerably higher. The experimental results are given under tests 18 and 20 in Table 4. For the small gap, the speeds tested do not exceed the large-amplitude theoretical flutter speed of 116 ft/s, so it is difficult to decide whether to characterize the motion as incipient flutter or as a stable limit cycle. As was observed with the other clamp location, the instability is amplitude-sensitive at the larger gap. Here it does appear that a stable limit cycle occurs, at least for the limited range of speeds tested. Figures 4 and 5 illustrate the behavior observed on chart recordings for divergent flutter and limit-cycle flutter, respectively.

With the plunge clamp at location C and a softening spring configuration, the experimental results are summarized by the data given for tests 14 and 15 in Table 4. With a small preload (test 14), the system resembles a linear system with the large-amplitude properties. As can be seen in Table 4, the data given for test 14 were obtained with only the tunnel turbulence for excitation. From these data it appears that a mild limit-cycle instability occurs near a speed of 119 ft/s at a frequency

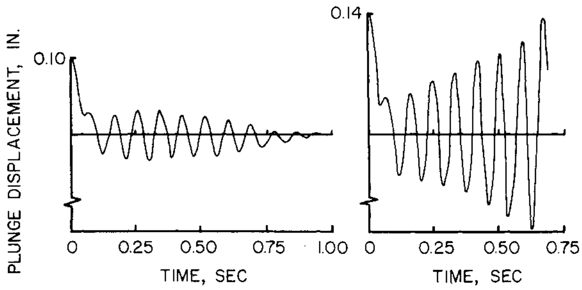

Fig. 6 Chart recordings of subcritical and supercritical response, $V = 128$ ft/s, test 13.

of 13.8 Hz. The theoretical large-amplitude values are 117 ft/s and 12.5 Hz. With a larger preload (test 15), the situation is much the same, except that higher speeds were reached, and the frequency is much closer to the theoretical small-amplitude value. This is to be expected, since the limit-cycle amplitudes did not exceed the preload static deflection. Unfortunately, the model was not plucked in these tests, so nothing can be said concerning the existence of an amplitude-sensitive instability. The small difference in theoretical small-amplitude and large-amplitude flutter speeds could also be a complicating factor, since it could easily be hidden by experimental uncertainties.

With the clamp at location D, this is not the case, since the theoretical difference here is 84 ft/s. The experimental results for a very small preload (test 19) indicate the existence of a limit-cycle amplitude-dependent instability at a speed and frequency closely corresponding to the theoretical large-amplitude values. No attempt was made to check the theoretical small-amplitude flutter speed of 200 ft/s because it was feared that the resulting instability would be so violent as to damage the model.

Time histories were also calculated in order to see if an amplitude-sensitive instability could be demonstrated theoretically. The configuration used for test 13 was chosen, with $V = 128$ ft/s. The experiment indicates that an initial plunge amplitude near 0.14 in. (or 0.030 in. at the gap) is necessary to induce flutter. This is illustrated in Fig. 6, which presents chart recordings of the plunge displacement for initial plunge displacements of 0.10 and 0.14 in. Theoretical time histories were obtained for a number of different initial plunge displacements. These time histories predicted that the critical value of the initial displacement was between 0.08 and 0.09 in. The theoretical frequency at an initial displacement of 0.09 in. was 11.4 Hz, which is lower than the experimental value of 12.1 Hz. An increase in frequency with initial displacement was observed theoretically, however, and the frequency for 0.14 in., which corresponds to the supercritical response in Fig. 6, was 11.9 Hz.

With linear plunge springs and a stiffening pitch spring (tests 22 and 23), a stable limit-cycle flutter was observed, once the linear low-amplitude flutter speed was exceeded. Table 4 shows that the limit-cycle amplitude was large enough to close the gap, and the frequency increased as the limit-cycle amplitude increased. Such behavior is expected with this type of nonlinearity, where a linear model with the high-amplitude stiffness value predicts a much higher flutter speed.

Before the conclusions are stated, some general observations are in order concerning the experimental procedures. In almost all of the tests where limit-cycle or divergent flutter was observed, the model would oscillate almost continuously at very low amplitudes at speeds slightly below the critical speeds identified in Table 4. The data presented for some of the tests with limit-cycle amplitudes (at the gap locations) of 0.002-0.008 in. are representative of this phenomenon. This motion is felt to be the response of the critical flutter mode to tunnel turbulence—which is, of course, very lightly damped as the flutter speed is approached. The existence of divergent flutter is presumed to be established when the motion resulting either from the tunnel turbulence or excitation by hand (plucking) increases in amplitude until the model must be restrained to prevent damage. Therefore there is no way of knowing if a limit-cycle motion exists at an amplitude that exceeds the critical amplitude. A limit cycle is presumed to exist if a stable oscillation is reached at an amplitude considerably greater than that observed in the low-damping, or incipient-flutter, regime. It is recognized that the procedures followed to test the existence of a limit cycle could be improved. In particular, the model can be given different initial plunge displacements. If there is a limit cycle, the same limit-cycle amplitude and frequency will be observed for all initial amplitudes greater than the critical amplitude. Also, there is a need for more precise release of the model. To date, the model has simply been displaced and released by hand. A more abrupt release, obtained by mechanical displacement and release of the model, would produce an initial condition closer to the theoretical initial condition used (nonzero plunge displacement only). Finally, it must be noted that the effects of the plunge bias observed in the experiments have not been accounted for in the theoretical model of the system. This bias can be easily accounted for by introducing an additional plunge force, linearly dependent upon dynamic pressure, into the equations of motion. This force will not affect the stability of the system, except possibly for the bias it introduces into the relationship between the nonlinear plunge spring forces and the plunge displacements. For example, the critical amplitudes for an amplitude-sensitive instability might be different in the positive and negative plunge directions. No effort was made to measure these differences experimentally.

Concluding Remarks

One of the principal goals of this project was to design and construct a typical-section flutter model with the following characteristics: 1) properties of nominal linear configuration well defined; 2) easily introduced and measurable nonlinear properties; 3) accurate measurements of all states available; and 4) nonlinear behavior easily distinguishable from linear behavior.

This goal has, by and large, been met. For example, damping, which is difficult to measure, has been minimized in the model by minimizing the sources of dissipative forces. Subcritical and supercritical response data have been taken for a number of configurations. Amplitude-sensitive instabilities, resulting in either divergent flutter or a limit-cycle oscillation, have been obtained experimentally. Phenomena such as these are clearly the results of the nonlinearities that have been introduced.

A theoretical model of the system has been developed that predicts the linear stability characteristics very well. And, in at least one instance, the existence of a divergent, amplitude-sensitive instability has been confirmed by direct numerical simulation (time histories). This model can be improved by refinement of the values used for the aerodynamic lag parameters (see Refs. 7 and 8).

There is much additional work that is planned, including more systematic nonlinear tests with a wider variety of nonlinear configurations, and theoretical correlations involving both direct numerical simulation and nonlinear stability analyses. In particular, the following tasks will be undertaken:

1) Conduct additional nonlinear tests with a device that will provide more precise initial conditions. Obtain more data on amplitude-sensitive instabilities and limit cycles.

2) Complete the validation of the theoretical model by obtaining better estimates of the aerodynamic lag parameters. Either eliminate the experimental plunge bias or incorporate it in the theoretical model.

3) Investigate the feasibility of applying different theoretical techniques to analyze nonlinear flutter. Among the

techniques to be considered are the method of multiple scales[10,11] and a perturbation method based on Lie transforms.[12]

Acknowledgments

This work was accomplished by the sponsorship of the Naval Air Systems Command under Contract No. N00019-78-C-0018. Dr. A.R. Somoroff and Dr. D. R. Mulville were the technical monitors. The authors are indebted to Mrs. Heather Bagwell and Mrs. Mary Keirstead for their aid with programming and the numerical computations.

References

[1] Breitbach, E., "Effect of Structural Nonlinearities on Aircraft Vibration and Flutter," AGARD Report 665, Jan. 1978.

[2] Dailey, G., Oedy, R.J., and Werback, W.J., "A State-of-the-Art Review of Methods in Aeroelasticity and Structural Analyses for Guided Weapons," Paper 39, presented at the 10th Navy Symposium on Aeroballistics, Fredericksburg, Va., July 1975.

[3] Truxal, J.G., *Control System Synthesis,* McGraw-Hill, New York, 1955, Chap. 10.

[4] Laurenson, R.M. and Trn, R.M., "Flutter Analysis of Missile Control Surfaces Containing Structural Nonlinearities," AIAA Paper 79-0796, April 1979.

[5] Woolston, D.S., Runyan, H.L., and Byrdsong, T.A., "Some Effects of System Nonlinearities in the Problem of Aircraft Flutter," NACA TN 3539, Oct. 1955.

[6] Rock, S.M., "Transient Motion of an Airfoil: An Experimental Investigation in a Small, Subsonic Wind Tunnel," Guidance and Control Laboratory, Stanford University, Stanford, Calif. SUDAAR 513, May 1978.

[7] McIntosh, S.C. Jr., Reed, R.E. Jr., and Rodden, W.P., "An Experimental and Theoretical Study of Nonlinear Flutter," Nielsen Engineering & Research, Inc., Mountain View, Calif., TR 209, Oct. 1979.

[8] McIntosh, S.C. Jr., Reed, R. E. Jr., and Rodden, W.P., "An Experimental and Theoretical Study of Nonlinear Flutter," AIAA Paper 80-0791, May 1980.

[9] Rodden, W.P. and Stahl, P., "A Strip Method for Prediction of Damping in Subsonic Wind Tunnel and Flight Flutter Tests," *Journal of Aircraft,* Vol. 6, Jan.-Feb. 1969, pp. 9-17.

[10] Morino, L., "A Perturbation Method for Treating Nonlinear Panel Flutter Problems," *AIAA Journal,* Vol. 7, March 1969, pp. 405-411.

[11] Van Dyke, M.D., *Perturbation Methods in Fluid Mechanics* (annotated ed.), Parabolic Press, Stanford, Calif., 1975.

[12] Kamel, A.A., "Perturbation Method in the Theory of Nonlinear Oscillations," *Celestial Mechanics,* Vol. 3, Dec. 1970, pp. 90-106.